

University of Rhode Island

DigitalCommons@URI

---

Civil & Environmental Engineering Faculty  
Publications

Civil & Environmental Engineering

---

6-2014

## Cold In-Place Recycling as a Sustainable Pavement Practice

Kang-Won Wayne Lee

*University of Rhode Island, leekw@uri.edu*

Max Mueller

*University of Rhode Island*

Ajay Singh

*University of Rhode Island*

Follow this and additional works at: [https://digitalcommons.uri.edu/cve\\_facpubs](https://digitalcommons.uri.edu/cve_facpubs)

---

### Citation/Publisher Attribution

Lee, K.W. W., Mueller, M., & Singh, A. (2014). Cold In-Place Recycling as a Sustainable Pavement Practice. *Journal of Civil Engineering and Architecture*, 8(6): 680-692. doi: 10.17265/1934-7359/2014.06.002  
Available at: <http://dx.doi.org/10.17265/1934-7359/2014.06.002>

This Article is brought to you by the University of Rhode Island. It has been accepted for inclusion in Civil & Environmental Engineering Faculty Publications by an authorized administrator of DigitalCommons@URI. For more information, please contact [digitalcommons-group@uri.edu](mailto:digitalcommons-group@uri.edu). For permission to reuse copyrighted content, contact the author directly.

---

## Cold In-Place Recycling as a Sustainable Pavement Practice

Creative Commons License



This work is licensed under a [Creative Commons Attribution-Noncommercial 4.0 License](https://creativecommons.org/licenses/by-nc/4.0/)



# Cold In-Place Recycling as a Sustainable Pavement Practice

Kang-Won Wayne Lee, Max Mueller and Ajay Singh

*Department of Civil and Environmental Engineering, University of Rhode Island, Kingston 02881, USA*

**Abstract:** Pavement rehabilitation and reconstruction methods with CIR (cold in-place recycling) are alternatives that can effectively reduce the high stresses and waste produced by conventional pavement strategies. An attempt was made to predict the performance, particularly low-temperature cracking resistance characteristics of CIR mixtures. These were prepared with the mix design procedure developed at the URI (University of Rhode Island) for the FHWA (Federal Highway Administration) to reduce wide variations in the application of CIR mixtures production. This standard was applied to RAP (reclaimed asphalt pavement) to produce CIR mixtures with CSS-1h asphalt emulsion as the additive. By adjusting the number of gyrations of the SGC (Superpave gyratory compactor) for compaction, the field density of 130 pcf was represented accurately. To secure a base line, HMA (hot mix asphalt) samples were produced according to the Superpave volumetric mix design procedure. The specimens were tested using the IDT (indirect tensile) tester according to the procedure of AASHTO T 322 procedure at temperatures of -20, -10 and 0 °C (-4, 14, and 32 °F, respectively). The obtained results for the creep compliance and tensile strength were used as input data for the MEPDG (mechanistic empirical pavement design guide). The analysis results indicated that no thermal or low-temperature cracking is expected over the entire analysis period of 20 years for both HMA and CIR mixtures. Thus, it appears that CIR is a sustainable rehabilitation technique which is also suitable for colder climates, and it is recommended to conduct further investigation of load-related distresses such as rutting and fatigue cracking.

**Key words:** Cold in-place recycling, sustainable pavement, asphalt pavement, pavement rehabilitation and reconstruction, Superpave gyratory compactor, indirect tensile test.

## 1. Introduction

Roadways are exposed to various loadings and stresses that reduce their serviceability like other infrastructures. Traffic as well as environmental stresses wear out pavement structures. Despite their consideration in the design and construction process, distresses can usually be expected to show in the pavement surfaces. The most efficient means to deal with these distresses and wearing appears to be to rehabilitate the pavement at a point where its condition can be improved with a reasonable amount of resources. This could be an adequate maintenance practice in order to avoid expensive reconstruction, and it needs to be planned throughout the expected pavement service period.

Whenever rehabilitation or reconstruction measures are not avoidable, procedures to rebuild parts of the pavement structure are necessary. Layers of the roadway are milled up to a determined depth, which can include the surface or even the base course. Past and current practices often pursue the procedure of replacing the milled materials with virgin materials [1]. This requires great efforts in terms of purchasing and transporting new material which consumes time, energy and money [2]. Furthermore, the old material becomes waste, harming the environment and incurring further costs tied to disposal.

A method of reducing all these issues by considerable amounts is in-place recycling. This procedure allows the user to re-use materials that are already in the pavement. This process includes milling, screening and crushing of the broken pavement materials. Additives such as emulsified asphalt or fly ash are then incorporated [3]. This mixture is put back

---

**Corresponding author:** Kang-Won Wayne Lee, Ph.D., Prof., research fields: pavement and transportation engineering. E-mail: leew@egr.uri.edu.

in place and compacted. Finally, a protective overlay is placed above the recycled layer of asphalt concrete, which is typically HMA (hot mix asphalt) [4]. Therefore, multiple advantages arise from the lack of need for heating and for extensive transportation of the materials used and are as follows [5]:

- less trucking;
- conservation of materials, energy and time;
- preservation of the environment;
- cost reduction.

These advantages pose major incentives to promote and support in-place recycling and allow the roadway rebuilding procedure to be conducted in a sustainable way [6].

In-place recycling can be performed at different temperature levels. Cold recycling typically uses materials at ambient temperatures. Examples show that temperatures are at around 25 °C (77 °F). The absence of the necessity to heat up the material considered to be major advantages which are listed above. Furthermore, pollution in the form of smoke, heat and noise is reduced. Thus, in-place recycling is an approach for green highways and streets. Less time is needed for cooling off, therefore allowing sooner openings for traffic too.

What are still needed for a wide-spread application of this technique are standardized regulations for procedures, testing, and quality control [7]. Based on a standard mix design procedure developed under the leadership of the URI (University of Rhode Island), the present study deals with the prediction of performance of pavements with CIR (cold in-place recycling), particularly, low-temperature cracking resistance characteristics [8]. In order to be able to fairly evaluate the outcomes of the predictions and obtain comparable results, the predictions for the pavement structures involving recycled materials were compared to a pavement structure with virgin materials, in this case HMA, with the same boundary conditions. Even with varying thicknesses of different layers in the pavement structure, exposure to the same environmental

conditions ensures a fair comparison.

## 2. Current Status of Knowledge

The literature review comprised many fields of pavement engineering, starting from the specimen preparation, i.e., basic material handling, all the way to software-based predictions on the basis of analyzed test data [9]. This chapter will focus on the used emulsion, theoretical background of the conducted testing and the prediction tool.

### 2.1 Asphalt Emulsions

In general, “emulsified asphalt is simply a suspension of small asphalt cement globules in water, which is assisted by an emulsifying agent” [3]. As liquid asphalt is based on oil and does not dissolve in water, a chemical agent is needed to disperse the liquid asphalt in water. It forms droplets with a diameter ranging from 1 µm to 10 µm [10].

CSS-1h emulsions are usually a good choice for CIR projects. The slow setting rate is suitable for this type of road construction. The number refers to the emulsion’s viscosity. In this case, the emulsion has a lower viscosity than a “2”. The “h” designates the use of harder base asphalt, which is usually the case.

### 2.2 Indirect Tensile Testing

When conducting the IDT (indirect tension) test, a cylindrical specimen with a diameter of 150 mm (6 in) and a thickness of 38-50 mm (1.5-2 in) is exposed to a single load imposed perpendicularly to the longitudinal axis with a static support on the opposite side. Fig. 1 shows a front view of the specimen during the test.

It was found that the IDT test is able to represent the most critical location of a pavement under a wheel load [11]. Roque and Buttlar [12] stated that, “the critical location for load-induced cracking is generally considered to be at the bottom of the asphalt concrete layer and immediately underneath the load, where the stress state is longitudinal and transverse tension combined with vertical compression. The stress state in

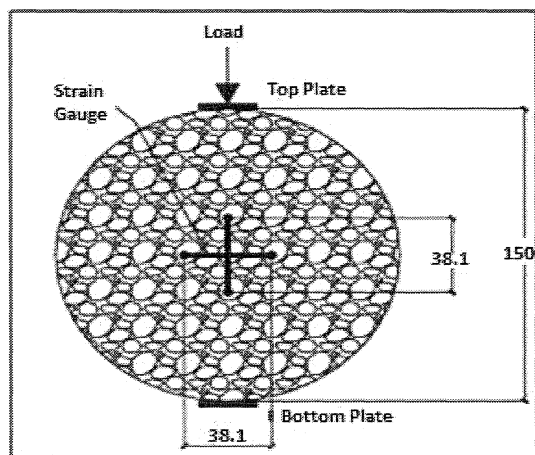


Fig. 1 IDT specimen and gauge location to determine creep compliance and tensile strength.

the vicinity of the center of the face of an indirect tension specimen is very similar to this stress state, except that tension is induced in one rather than two axes”.

According to Roque and Buttlar [12], the tensile stress along the vertical y-axis in the horizontal direction is constant, which also reflects the line along which failure can be expected once the tensile stress exceeds the tensile strength (Fig. 1).

The IDT test is conducted according to the AASHTO T 322 procedure [13]. Its purpose is to determine the creep compliance  $D(t)$  as well as the tensile strength  $S_t$  at low temperatures. Creep compliance is defined as “the time-dependent strain divided by the applied stress” [12] and therefore has the unit of the reciprocal of stress. A constant load is to be applied on the specimen for a duration of 100 (MEPDG (mechanistic empirical pavement design guide) input values) or 1,000 s (complete analysis). Not only does superpave mixture analysis specify the temperatures of  $-20$ ,  $-10$  and  $0^\circ\text{C}$  ( $-4$ ,  $14$  and  $32^\circ\text{F}$ , respectively), but also the input options for MEPDG are at these temperatures. In order to allow the specimen to cool down to the test temperature and establish an appropriate temperature distribution throughout the material, the sample has to remain inside the climate chamber at the test temperature for 2

$\pm 1$  h prior to testing.

During creep compliance testing, the deformations near the center of the specimen are recorded. The tensile strength test is to be performed immediately after the creep compliance test. Now the loading ram movement is required to be constant with a speed of 12.5 mm/min until the load sustained by the specimen decreases. This is regarded to as failure and the maximum load therefore is the failure load.

### 2.3 AASHTO Pavement M-E Guide

The MEPDG, subsequently AASHTO Pavement M-E Guide was developed based on results of the LTPP (long-term pavement performance) program. The LTPP program started a comprehensive experiment about pavements in service by monitoring more than 2,400 asphalt and Portland cement concrete roadways across the United States and Canada. The data obtained help to develop the algorithms for the new performance prediction software. With the weather history known about the location where the future pavement is to be constructed, the pavement structure can be entered into the program. Then, the program output is a prediction of the serviceability of the roadway that can be expected under the given boundary conditions. MEPDG combines a variety of sub-programs that each treat different distresses such as rutting, fatigue cracking and thermal cracking.

TC MODEL is the program which analyzes the stresses due to low temperatures and is able to quantify the thermal distresses. It should be noted at this point that “TC MODEL does not consider traffic effects” [14]. This program is very user-friendly, as it offers a convenient way to enter the data input. It simplifies the problem by using linear elastic fracture mechanics in a one-dimensional stress evaluation model. Newer software aims to treat this problem with nonlinear finite element analysis engines. This allows for better reliability of the predictions due to a more accurate mathematical representation of the problem. This software is still under development for the full-scale

deployment [15].

### 3. Asphalt Pavement Materials

The primary objective of this study was the evaluation of the performance of a CIR material for rehabilitation or reconstruction projects. A base line was established with HMA first.

#### 3.1 HMA Specimens

HMA represents the current practice of road construction, and consists of mineral aggregates and asphalt binder. Specimens with four different binder contents from 5.5% to 7.0% with increments of 0.5% were tested, and the OBC (optimum binder content) was determined at the in-service air void content of 4.0%.

A loose (uncompacted) sample with a mass of approximately 1,000 g (2.2 lbs) was used to determine the theoretic maximum specific gravity according to the procedure of AASHTO T 209 [13]. Specimens with different binder contents were compacted with the SGC (Superpave gyratory compactor) maximum number of gyrations, i.e., 175. It should be noted that the final compaction level is important for calculation purposes only, but not for testing. 175 gyrations would compact the specimens to a point where they would be denser than in the field and would not represent field conditions accurately, since the number of gyrations for design purposes would be 100 according to the procedure of AASHTO R 35 [13]. The obtained test results were only used for back-calculating purposes and not for performance testing.

The compacted specimens were then tested for their bulk SG (specific gravity) ( $G_{mb}$ ) and water absorption according to the procedure of AASHTO T 166 [13]. The bulk SG after every gyration can be estimated because the specimen's mass is known and the gyratory compactor yields the height of the specimen after every gyration in the compaction mold of known dimensions. By dividing the mass by the calculated volume and the density of water at 4.0 °C (0.999972 g/cm<sup>3</sup>), the

estimated bulk SG ( $G_{sb,est}$ ) can be computed. A correction factor  $C$  is introduced to obtain the corrected bulk SG ( $G_{sb,corr}$ ). It is determined and applied to every gyration according to Eqs. (1) and (2) [16].

$$C = \frac{G_{mb,measured}}{G_{mb,est} (N = 175 \text{ gyrations})} \quad (1)$$

$$G_{mb,corr} = G_{mb,measured} \cdot C \quad (2)$$

By dividing the corrected bulk SG by the theoretical maximum SG, the compaction level as a percentage of the maximum theoretical SG is computed. This calculation was done for duplicate specimens at four binder contents. Then, the binder content is plotted against the averaged air void contents. The results are shown in Fig. 2.

Finally, the OBC at an air void content of 4.0% was determined graphically and numerically to be 5.8%. Therefore, the specimens for the planned indirect tensile testing were produced with this OBC. Also, compaction was accomplished with 100 designs instead of 175 maximum gyrations.

#### 3.2 CIR Mixtures

RAP (reclaimed asphalt pavement) was acquired from a construction site of Rhode Island Route 3. Unfortunately, the material was stored uncovered for an unknown amount of time, and the influence of aging, oxidation and freezing, especially on the binder, may have been significant. However, since another source was not available, the RAP was used despite concerns over different properties from fresh one.

In this study, CSS-1h emulsion was used. According to the CIR mix design procedure which was developed by a URI research team [8], the optimum emulsion and water content needed to be determined. The process was carried out by first keeping the water content constant and varying the emulsion content. For the determination of the optimum content, the unit weight is the parameter to be compared to field conditions. Either the maximum value or, if a maximum cannot be

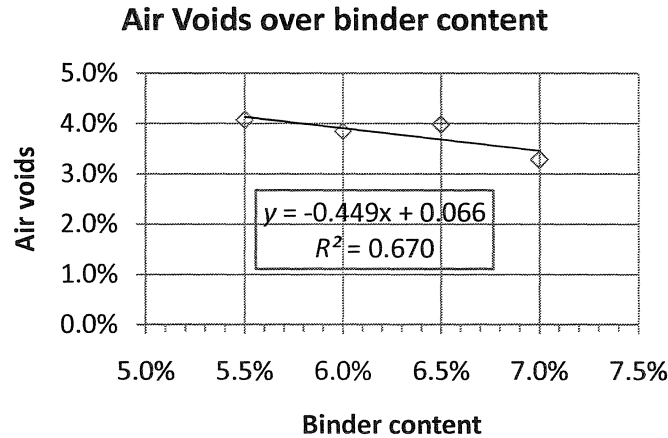


Fig. 2 Averaged air voids over binder content.

determined, the best representation of field condition should be chosen. Before any specimen can be produced, the appropriate number of gyrations for compaction needs to be determined. The URI procedure states that, “The load shall be applied for the number of gyrations that will result in achieving densities similar to those found in the field.” Therefore, a method was used that is somewhat similar to the determination of the amount of air voids for HMA materials [8]. It is based on representing field density, and the value of previous URI study, i.e., 130 pcf was used [17]. Following steps were used in this study:

- determine the mass of the sample (aggregate + water + emulsion);
- compact with 175 gyrations (like HMA) [7];
- calculate estimated bulk SG after every gyration;
- measure bulk SG after 175 gyrations (experiment);
- correction factor  $C = (\text{measured bulk SG after 175 gyrations}) / (\text{estimated bulk SG after 175 gyrations})$ ;
- multiply bulk SG after every gyration by  $C$  to obtain corrected bulk SG;
- find field density;
- divide corrected bulk SG by field density;
- look for 100.0%.

The test specimen for this procedure was made with

a water content of 3.0% and an emulsion content of 1.0%. Results showed that 116 gyrations are adequate for field density reproduction.

For any set of emulsion and water contents, 9,000 g of RAP were used. This was because duplicate specimens for bulk SG determination with about 4,000 g each were needed along with one sample for theoretical maximum SG determination (approx. 1,000 g). To ensure sufficient mass, 9,000 g for the RAP was chosen because emulsion and water still had to be added, which lead to a mass of more than 9,200 g before curing [5]. For the determination of the OEC, emulsion contents varied from 0.5% (of total mix mass) to 2.0% with increments of 0.5%, while the water content stayed constant at 3.0%.

After production, specimens were put in an oven at a temperature of 60 °C (140 °F) for a period of 24 h for curing. This time was needed for the water to leave the specimen [8].

While the bulk SG specimens were being cured, the theoretical maximum SG of uncompacted specimens was determined. This was conducted according to the procedure of AASHTO T 209 [13]. After curing, bulk SG testing was performed, again according to the procedure of AASHTO T 166 [13]. Fig. 3 shows the unit weight with respect to emulsion content. The  $R^2$

error is in reference to a parabolic regression curve computed by the spreadsheet program.

In one aspect, the regression fits the data points very well which is indicated by the  $R^2$  value above 0.99 in both cases. However, the behavior of the curve was somewhat different than expected since it indicated that a higher unit weight was achieved using less emulsion. A similar behavior was observed [8] and a solution corresponding to the applied mix design procedure was applied.

Due to the highly variable nature of RAP materials and their mixture with emulsion and water, the relationship between unit weight and emulsion content, as described earlier, occasionally does not hold true for CIR mixtures. Such a case occurred with the Kansas mixture. The highest unit weight was achieved at the lowest emulsion content of 0.5%. However, 0.5% emulsion does not supply enough asphalt to properly coat the RAP particles. Under such conditions, the OEC should be selected at the emulsion content that produces the same unit weight as found in the field.

In this study, the same option was chosen. Due to the close fit of the regression curve, it could be used to numerically determine at which emulsion content a unit weight of 130 pcf was achieved. Thus, the optimum emulsion content was determined to be 0.7%.

With the optimized emulsion content, the next step was to determine the OWC (optimum water content).

This was very similar to the previous step with the exception that the emulsion content was kept constant at the optimum level while the water content was varied. Again, four sets of specimens were produced with 116 gyrations. However, the water contents were varied from 2.0% to 3.5%. The results are shown in Fig. 4.

While the behavior was expected to be less erratic, one maximum point could be identified easily to determine the optimum water content to be 3.0%.

#### 4. IDT (Indirect Tensile) Testing

##### 4.1 Specimen Preparations

A testing machine, Instron® 5582 was available in the RITRC (Rhode Island Transportation Research Center) laboratory at URI. An attempt was made to calibrate the machine. A malfunction was found in data acquisition system. Suitable new parts that would work with the machine were identified, but unfortunately the delivery and complete installation of the new software was too late for this project to take effect. Therefore, another way of testing needed to be found. Fortunately, the UConn (University of Connecticut) provided the required testing system for this project.

The superpave cylindrical samples have a height of about 110 mm (4.3 in), thus two IDT specimens with the required height could be produced. Due to the quality of the saw, a high level of accuracy could be

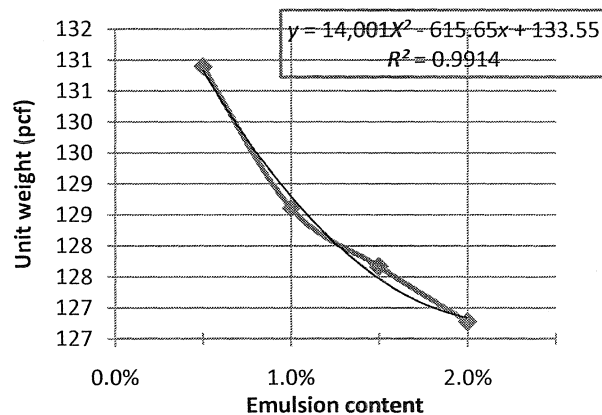


Fig. 3 Determination of OEC at 3.0% water content.



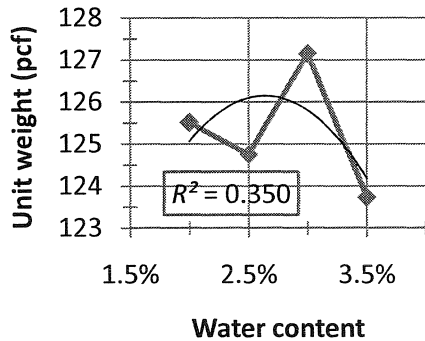


Fig. 4 Determination of OWC at 0.7% emulsion content.

maintained. In total, eight different specimens for each material were produced with thicknesses in the range of 41 mm to 44 mm. These met the requirement of the procedure of T 322, which are 38-50 mm [13]. It was observed that the different behavior of the materials could be seen even during specimen preparation. The fine materials of the recycled samples were less strongly integrated into the material and therefore chipping was increased during sawing. In order to still obtain usable specimens, care had to be taken to saw the specimens fast enough to minimize wobbling of the blade and at the same time slow enough not to rip out particles instead of cutting through them.

At least one day was required after sawing as the specimens had to be dried. Subsequently, metal mounting buttons were glued onto the specimens. For testing, strain gauges were attached to them magnetically to detect the horizontal and vertical deflection of the sample in the center of the specimen. After gluing the buttons to the specimens, they were ready for testing.

#### 4.2 IDT Testing Content

Testing had to be conducted at different temperatures. To ensure an appropriate temperature distribution over the entire cross-section of the specimens, keeping the specimens at test temperatures for  $3 \pm 1$  h before testing was mandatory. The entire testing procedure was conducted according to the

procedure of AASHTO T 322 [13].

While the load was kept at a constant magnitude, the deflections were measured for both faces of the specimen. This is intended to reduce influences on the obtained measurements due to material in homogeneities by allowing the user to average them. After this testing phase, the load was removed. Although the specimen was not destroyed, it exhibited permanent deformation. However, it can still be used for the tensile strength test, as can be seen in the standard test method [13]. In this test, the loading ram had to maintain a constant movement of 12.5 mm/min (0.5 in/min), while only the imposed load needed to be measured. The deflections did not matter at this time. Since this test destroys the specimen, the strain gauges were removed to prevent damage that might have occurred due to the specimen's collapse.

The ram movement must be maintained until the load sustained by the specimen starts to decrease. This is regarded as failure, and the maximum load was used. When testing materials at different temperatures, it was observed that the temperature had a significant influence on the behavior. The lower the temperature, the more brittle failure occurred. While the material allowed some ductile deformation before completely falling apart at freezing point. At  $-20^{\circ}\text{C}$  ( $-4^{\circ}\text{F}$ ) there was mainly one sudden, loud crack, and the specimen collapsed.

#### 4.3 Data Analysis

##### 4.3.1 Creep Compliance, $D(t)$

The horizontal and vertical deformations at the analyzed temperature were averaged and normalized in order to compare them. This was accomplished using Eqs. (3) and (4) [13].

$$\Delta X_{n,i,t} = \Delta X_{i,t} \cdot \frac{b_n}{b_{avg}} \cdot \frac{D_n}{D_{avg}} \cdot \frac{P_{avg}}{P_n} \quad (3)$$

$$\Delta Y_{n,i,t} = \Delta Y_{i,t} \cdot \frac{b_n}{b_{avg}} \cdot \frac{D_n}{D_{avg}} \cdot \frac{P_{avg}}{P_n} \quad (4)$$

where,

$\Delta X_{n,i,t}$ —normalized horizontal deformation of specimen  $n$  for face  $i$  at time  $t$  (mm);

$\Delta Y_{n,i,t}$ —normalized vertical deformation of specimen  $n$  for face  $i$  at time  $t$  (mm);

$\Delta X_{i,t}$ —measured horizontal deformation of specimen  $n$  for face  $i$  at time  $t$  (mm);

$\Delta Y_{i,t}$ —measured vertical deformation of specimen  $n$  for face  $i$  at time  $t$  (mm);

$b_n, D_n, P_n$ —thickness, diameter, creep load of specimen  $n$ ;

$b_{avg}, D_{avg}, P_{avg}$ —average thickness, diameter, creep load of all replicate specimens at this temperature.

Since all specimens have a diameter of 150.0 mm,  $D_n/D_{avg}$  is 1. In the test method,  $\Delta X$  and  $\Delta Y$  are treated as arrays. In this study, this is achieved by calculating single values in a table in the spreadsheet software. After executing these equations, normalized deformations are obtained that enable the user to directly compare the deflections of all three specimens to one another.

If the average was determined with all six curves or arrays, the accuracy would decrease due to these two curves that deviate from the mean value significantly. As an approach to this problem, the trimmed mean is used. A percentage of all measurements is chosen to be “cut off” or trimmed from the top and bottom of the numerically ranked array before calculating the arithmetic mean.

The average horizontal and vertical deformations for every face are needed in order to determine the ratio of the horizontal to vertical deformations  $X/Y$ , Poisson’s ratio  $\nu$ , and a coefficient,  $C_{cpl}$ , needed for the calculation of the creep compliance. The average deformations occur after half the total creep time and are obtained using Eqs. (5) and (6) from the procedure of AASHTO T 322 [12].

$$\Delta X_{a,i} = \Delta X_{n,i,t_{mid}} \quad (5)$$

where,

$\Delta X_{a,i}$ —average horizontal deformation for face  $i$ ;

$\Delta X_{n,i,t}$ —normalized horizontal deformation at a time

corresponding to half the total creep test time for face  $i$ , here  $t = 500$  s.

The vertical deformations were obtained by applying the same calculations to the  $\Delta Y$  values. Then, the trimmed mean of the deflections  $\Delta X_i$  and  $\Delta Y_i$  needed to be obtained. For this, the six  $\Delta X_{a,i}$  and  $\Delta Y_{a,i}$  values were ranked numerically and the highest and lowest values were disregarded. The average of the middle four values was determined, according to Eq. (6).

$$\Delta X_t = \frac{\sum_{j=2}^5 \Delta X_{r,j}}{4} \quad (6)$$

where,

$\Delta X_t$ —trimmed mean of horizontal deformations;

$\Delta X_{r,j}$   $\Delta X_{a,i}$ —values in ascending order.

The ratio of the horizontal to vertical deformations  $X/Y$  was computed according to Eq. (7).

$$\frac{X}{Y} = \frac{\Delta X_t}{\Delta Y_t} \quad (7)$$

Consequently,  $C_{cpl}$  and  $\nu$  were determined using Eqs. (8) and (10), respectively.

$$C_{cpl} = 0.6354 \cdot \left(\frac{X}{Y}\right)^{-1} - 0.332 \quad (8)$$

while Eq. (9) must be true.

$$\left[ 0.704 - 0.213 \left( \frac{b_{avg}}{D_{avg}} \right) \right] \leq C_{cpl} \leq \left[ 1.566 - 0.195 \left( \frac{b_{avg}}{D_{avg}} \right) \right] \quad (9)$$

$$\nu = -0.10 + 1.480 \left( \frac{X}{Y} \right)^2 - 0.778 \left( \frac{b_{avg}}{D_{avg}} \right)^2 \left( \frac{X}{Y} \right)^2 \quad (10)$$

It may be noted that Poisson’s ratio  $\nu$  should always be between 0.05 and 0.50 [12]. The calculations were carried out in a spreadsheet program (Microsoft Excel ©). They were performed for all temperatures for both mixtures.

Based on the trimmed mean of the deflections (deflection arrays)  $\Delta X_{m,t}$  with respect to variable time  $t$  following the same numerical ranking for the average deformations in Eq. (6), the creep compliance  $D(t)$  can

finally be computed using Eq. (11).

$$D(t) = \frac{\Delta X_{tm,t} \cdot D_{avg} \cdot b_{avg}}{P_{avg} \cdot GL} \cdot C_{cpl} \quad (11)$$

where,

$D(t)$ —creep compliance (1/TPa);

$GL$ —gauge length (0.038 for 150 mm specimen).

This formula allows the computation of the creep compliance for any time recorded, in the present study every half-second. The simulation program, MEPDG, requires the creep compliance only at certain time points. For greater precision of the requested data points  $\Delta X_{tm,t}$ , the results were averaged over the surrounding 5 time points.

In summary, Table 1 was prepared as input material parameters for MEPDG analysis. As expected, CIR mixture has a higher compliance than HMA, because the former has lower modulus than the latter.

#### 4.3.2 Tensile Strength ( $S_t$ )

The creep testing is not a destructive test, however, permanent deformation is exhibited due to the viscoelastic reaction to a permanent load. The tensile strength test damages the specimen entirely which is why this test must, of course, be performed after the creep compliance test. AASHTO procedure T 322 schedules the strength test immediately after the creep compliance test but allows an unloading phase in between [13]. In the present study, this was necessary to remove the strain gauges to prevent damage to them as a result of specimen collapse.

The specimen is aligned in the same way as for the compliance test, but this time the loading piston is to

move at a constant speed of 12.5 mm/min. During testing only the sustained load is measured until a decrease is detected. This may or may not come along with a brittle collapse of the sample, but the maximum load is interpreted as the failure load and is used to determine the tensile strength. When the failure load is known, Eq. (12) allows computation of the tensile strength [13].

$$S_{t,n} = \frac{2 \cdot P_{f,n}}{\pi \cdot b_n \cdot D_n} \quad (12)$$

where,

$S_{t,n}$ —tensile strength of specimen  $n$  (GPa);

$P_{f,n}$ —failure load of specimen  $n$ .

Although the tensile strengths were obtained for all temperatures, only the results at -10 °C (14 °F) are significant for the program. While HMA mixtures collapsed at an average stress of 858 psi, CIR specimens failed at an average stress of 97 psi, which means a reduction of almost 90%. However, strength of 97 psi is strong enough as base materials.

## 5. Performance Prediction of Both Mixtures

The final step of performance prediction would be using the obtained data for a fictional project to evaluate the performance of the CIR mixture comparatively. It includes the input to the model and program for the selected boundary conditions of the site. Consequently, the outputs of the program would include resistance to low temperatures cracking and would be interpreted to formulate recommendations.

**Table 1** Creep compliance of both mixtures with respect to creep time  $t$ .

Creep time $t$ (s)	-20 °C HMA	-20 °C CIR	-10 °C HMA	-10 °C CIR	0 °C HMA	0 °C CIR
0	8.97389E-08	9.41206E-07	4.13707E-07	8.54305E-07	5.21493E-07	2.55396E-06
1	9.63726E-08	9.69910E-07	4.57243E-07	9.22309E-07	6.20040E-07	2.73292E-06
2	1.02322E-07	1.00329E-06	4.91514E-07	9.63768E-07	7.00792E-07	2.88960E-06
5	1.18006E-07	1.07410E-06	5.55092E-07	1.04849E-06	8.78080E-07	3.13043E-06
10	1.36596E-07	1.15122E-06	6.26694E-07	1.13398E-06	1.08040E-06	3.39047E-06
20	1.66465E-07	1.25605E-06	7.29301E-07	1.24203E-06	1.35649E-06	3.73268E-06
50	1.99880E-07	1.46296E-06	9.41392E-07	1.44683E-06	1.94403E-06	4.35663E-06
100	2.45938E-07	1.70172E-06	1.19195E-06	1.67104E-06	2.56138E-06	5.00597E-06

### 5.1 Input for TCMODEL and MEPDG

The MEPDG software offers a user-friendly input framework, characterized by a checklist layout. Each bullet point allows the adjustment of parameters for general information, traffic, climate and pavement structure.

For this project a “minor arterial rural highway” was selected: Rhode Island Route 2 leads from South Kingstown to North Kingstown [18]. A section of the road in the southern part of the State was chosen since from that area a report offers a variety of data for traffic and subgrade soil information. The study was conducted by a URI research team for the RIDOT (Rhode Island Department of Transportation).

In terms of the traffic amounts and distributions, it may be noted that thermal cracking is not load-related and does not depend on the amount of vehicles for this project. However, the programs require a completed set of information for any project, so the traffic amount of 1,346 AADTT (annual average daily truck traffic) was entered [18].

The climate plays a very important role for this distress. In MEPDG, the climate files are created based on the history that is known for weather stations in the vicinity of the project site. There are three stations in Rhode Island: Westerly, Newport and Providence. Newport, RI, is located on an island, and is also rather far away from the planned location. In addition, climate data from stations in neighboring States were available and were used for improved accuracy.

Next to the weather data, the location for which the data are to be interpolated needs to be entered. As shown, a position was chosen in the southern part of the State, its coordinates are N 41.52°, E 71.55°. The elevation is approximately 220 ft; both information were found using “Google Earth”. The depth of water table was entered as 10 ft [19].

Next, the pavement structure needs to be given to the software. The bottom layer is subgrade soil classified

by AASHTO standards as A-1-b, i.e., that a maximum of 50 and 25% of the aggregate would pass the No. 40 and No. 200 sieves, respectively [20]. The resilient modulus was 14,300 psi [18]. It is semi-infinite while the above layers are assigned finite thicknesses. The layer above the subgrade is granular subbase with a thickness of 12 in, as it is common in Rhode Island for a fill or embankment section. In the case of cut or excavation section, 18 in would be appropriate.

The base and surface courses need to be provided in the prediction software. This is the point where MEPDG, unfortunately, limits the possibilities to enter a pavement that would accurately reflect the way CIR is supposed to be used in reality. After application of CIR and curing, protection is required for “the surface of the CIR-treated material by either a surface wearing course, such as a seal or HMA overlay” [21]. Therefore, CIR would most likely be applied in combination with HMA. However, the program allows entering of only one set of creep compliance and strength test data for all bituminous layers of the entire setup, which prevents pavement structures that comprise layers of both HMA and CIR. So for comparison reasons, basically the two bituminous layers are entered with the creep compliance and tensile strength results from HMA in one case and from CIR in the other case. As it is practice in Rhode Island for deep strength pavements, the base and surface courses have thicknesses of 5 in and 2 in, respectively. In addition, a third setup was simulated with a base course thickness of only 2 in. This, of course, must never be used in reality. However, it is intended to reveal how a very thin course of CIR mixture would perform in terms of thermal cracking.

### 5.2 Prediction Results and Interpretation

After simulating all three different cases, summaries of distresses revealed that none of the cases are expected to exhibit any distresses over the entire analysis period of 20 years. Not even the third case, where the pavement is by far too thin, showed any

distresses. As an example, the output for the distresses of the pavement including CIR mixtures with a base course thickness of 5 in is shown in Table 2.

This is a rather unexpected result. Especially because of the observations about the bonding forces between the smaller particles of the material which appeared weaker than the HMA, apparently this property does not affect the distress of thermal cracking. It can be expected to affect the performance for a variety of load-related distresses such as longitudinal or alligator cracking; however, this was not within the scope of this project but is rather recommended to be analyzed in future research.

The question of the performance cannot be answered entirely with the result that neither material will crack at the simulated weather conditions. Still, the result that CIR material performs very well in a climate found in the south of Rhode Island is more than desirable and supports this approach towards a more sustainable reconstruction practice immensely.

How can a CIR mixture with a tensile strength of less than 12% of HMA's strength perform just as well? Apparently, not only the tensile strength, but the material's behavior before failure plays a significant role for cracking. This distress is not load-, but temperature-related. The stresses do not arise from imposed loads that need to be sustained, but rather from shrinkage. As mentioned earlier, the creep compliance is a measure of strain over stress. The creep compliances over time in Table 1 reveal for both materials that CIR exhibits a more ductile behavior, i.e., allows more deflection. As both mixtures are exposed to the same climatic situations, they both do not show temperature-related distresses, but behave differently. CIR mixtures reduce stresses by allowing higher deflections. HMA mixtures behave more brittle and deflect less, but do not fail because the tensile strength is higher than the actual stresses.

In summary, these results represent a more than desirable result for the analyzed problem. Thermal

**Table 2 Simulation output.**

Pavement age		Month	Longitudinal cracking CIR (ft/mi)	Longitudinal cracking HMA (ft/mi)	Alligator cracking CIR (%)	Alligator cracking HMA (%)	Transverse cracking CIR (ft/mi)	Transverse cracking HMA (ft/mi)
Mo	yr							
1	0.08	August	85	0.04	0.31	0.0011	0	0
12	1.00	July	1,600	0.39	2.38	0.0067	0	0
24	2.00	July	3,520	1.19	4.90	0.0147	0	0
36	3.00	July	4,740	1.88	6.95	0.0211	0	0
48	4.00	July	5,800	2.77	9.07	0.0279	0	0
60	5.00	July	6,490	3.75	11.00	0.0349	0	0
72	6.00	July	7,150	4.84	13.00	0.0421	0	0
84	7.00	July	7,670	5.98	15.00	0.0493	0	0
96	8.00	July	8,100	7.34	17.10	0.057	0	0
108	9.00	July	8,450	8.82	19.10	0.0649	0	0
120	10.00	July	8,730	10.7	21.20	0.0738	0	0
132	11.00	July	8,920	12	22.80	0.0811	0	0
144	12.00	July	9,090	13.7	24.50	0.089	0	0
156	13.00	July	9,220	15.3	26.10	0.0971	0	0
168	14.00	July	9,350	17.1	27.70	0.105	0	0
180	15.00	July	9,470	19	29.30	0.114	0	0
192	16.00	July	9,570	21.1	30.90	0.122	0	0
204	17.00	July	9,660	23.3	32.60	0.131	0	0
216	18.00	July	9,740	26	34.20	0.142	0	0
228	19.00	July	9,800	28	35.50	0.15	0	0
240	20.00	July	9,860	30.3	36.90	0.159	0	0

cracking of this type of recycled pavement material is of such a low extent that it can be recommended, although more works in terms of performance regarding load-related distresses are necessary.

## 6. Conclusions and Recommendations

As a pavement rehabilitation alternative, the CIR mixture was evaluated. Specimens were produced using a rational mix-design with SGC. IDT testing was also performed at  $-20^{\circ}\text{C}$ ,  $-10^{\circ}\text{C}$  and  $0^{\circ}\text{C}$ , and compliances and tensile strengths were determined as input parameters for TCMODEL and MEPDG. Although it revealed that the tensile strength of CIR mixtures was reduced by up to 90%, the creep deflection was increased allowing the CIR mixtures to increase strain at a given load. The simulated results showed that no significant thermal cracking is expected to occur over the entire analysis period of 20 years. Thus, the results support CIR as a viable option for roadway rehabilitations. Through the reduced stresses to the environment and the people, CIR can provide a greener and more sustainable approach.

While the performed simulations were limited to exposure to Rhode Island climate, further investigations should be conducted for the severe weather conditions in other US states.

Further questions offer plenty of research possibilities regarding other types of distresses, variations for the additives and more.

Concerning the sample production, two major improvements are recommended. One of them is the production of more specimens to obtain an increased statistical reliability. In this project, the scope was limited, however, for future research projects more data are recommended. Also, a wet saw with a bigger blade could be better. It should be able to cut specimens with a diameter of 150 mm in one motion, i.e., without having to turn the specimen during cutting.

For the prediction, the used software simplifies the problem as it applies linear elastic fracture mechanics. Newer software is recommended for future use, e.g.,

“Low Temperature Cracking, TC Model” which contains non-linear approaches [22].

## References

- [1] Basic Asphalt Recycling Manual, AI (Asphalt Institute), NP-90 College Park, MD, 2011.
- [2] Asphalt Paving Technology, Association of Asphalt Paving Technologies, Charlestown, SC, 1992, pp. 304-332.
- [3] Understanding Emulsified Asphalts, Educational Series, AI (Asphalt Institute), Aug. 1979, pp. 1-5.
- [4] Mix Design Methods for Asphalt Concrete, AI (Asphalt Institute), College Park, MD, 1984.
- [5] In-Place Recycling, California Department of Transportation, Division of Maintenance, Feb. 19, 2008, <http://www.dot.ca.gov/hq/maint/FPMTAGChapter13-In-Place-Recycling.pdf> (accessed June 12, 2012).
- [6] S.A. Cross, E.R. Kearney, H.G. Justus, W.H. Chesher, Cold In-Place Recycling in New York States, Final Summary report, SPR Research Project, No. C-06-21, NYSERDA-TORC Contract No. 6764F-2, NYDOT, Albany, NY, 2010.
- [7] B.J. Coree, K. VanDerHorst, National Transportation Library, SUPERPAVE® Compaction[Online], 1998, <http://ntl.bts.gov/lib/9000/9000/9079/264superpave.pdf> (accessed Dec. 15, 2011).
- [8] K.W. Lee, T.E. Brayton, H. Milton, Development of Performance Based Mix Design for CIR (Cold In-Place Recycling) of Bituminous Pavements Based on Fundamental Properties, Federal Highway Administration, Washington, D.C., 2002.
- [9] M.S. Mamlouk, J.P. Zaniewski, Materials for Civil and Construction Engineers, 2nd ed., Upper Saddle River, Pearson Prentice Hall, NJ, 2006.
- [10] D. Walker, Asphalt Emulsions 101, The Magazine of Asphalt Institute, Mar. 2012, pp. 7-10.
- [11] T. Kennedy, F. Roberts, K.W. Lee, Evaluation of Moisture Effects on Asphalt Concrete Mixtures, Transportation Research Record, No. 911, TRB (Transportation Research Board), NAS (National Academy of Science), 1983, pp. 134-143.
- [12] R. Roque, W.G. Buttlar, The development of a measurement and analysis system to accurately determine asphalt concrete properties using the indirect tensile mode, Journal of the Association of Asphalt Paving Technologists 61, 1992, 304-332.
- [13] AASHTO Standard Method, American Association of State Highway and Transportation Officials, Washington, D.C., 2011.
- [14] M. Marasteanu, W. Buttlar, H. Bahia, C. Williams, Investigation of Low Temperature Cracking in Asphalt

- Pavements, Technical report, St. Paul, MN, 2007.
- [15] S. Leon, E.V. Dave, K. Park, Thermal cracking prediction model and software for asphalt pavements, in: T&DI Congress 2011, American Society of Civil Engineers, Chicago, 2011, pp. 667-676.
- [16] R.B. McGennis, R.M. Anderson, T.W. Kennesdy, M. Solaimanian, Background of Superpave Asphalt Mixture Design and Analysis, report No. FHWA-SA-95-003, Washington D.C., 1995.
- [17] K. Steen, Prediction of rutting and fatigue cracking of cold in-place recycling asphalt pavements using the vesys computer program, Master Thesis, University of Rhode Island, Kingston, 2001.
- [18] K.W. Lee, A.S. Marcus, K. Mooney, S. Vajjhala, E. Kraus, K. Park, Development of Flexible Pavement Design Parameters for Use with the 1993 AASHTO Pavement Design Procedures, FHWA-RIDOT-RTD-03-6, Rhode Island Department of Transportation, Providence, 2003.
- [19] Esri, ArcGIS Rhode Island Soil Permeability and Depth to Water Table[Online], 2011, <http://www.arcgis.com/home/webmap/viewer.html?services=4ca8feb53f504b3c9c2b8bcefe0afd4d> (accessed June 20, 2012).
- [20] H.N. Atkins, Highway Materials, Soils and Concretes, Prentice Hall, New Jersey, 2002.
- [21] FHWA, Cold In-Place Asphalt Recycling Application Checklist, US Department of Transportation, Washington, D.C., 2005.
- [22] E. Dave, W. Butllar, S. Leon, B. Behnia, G. Paulino, IIITC-low temperature cracking model for asphalt pavements, Road Materials and Pavement Design 14 (2) (2013) 57-58.